Solid Freeform Fabrication 2023: Proceedings of the 34th Annual International Solid Freeform Fabrication Symposium – An Additive Manufacturing Conference
Reviewed Paper

NOVEL WELDING STRATEGY IN HIGH DEPOSITION RATE LASER-ASSISTED DOUBLE-WIRE WELDING PROCESS WITH NONTRANSFERRED ARC

K. Biester*, N. Schwarz*, J. Hermsdorf* and S. Kaierle*

*Laser Zentrum Hannover e.V., 30419 Hannover, Germany

Abstract

Laser-assisted double wire welding with nontransferred arc melts material using an arc between two conveyed wires. Driven by gravity the molten metal drops onto the substrate. A laser beam is oscillated on the melt pool to bond the weld beads to the substrate without undercuts. Claddings at high deposition rates (11.6 kg/h) were performed with 316L on mild steel. The first welding strategy (AAA) is to weld adjacent beads (A) with a varied track spacing of 7 to 9 mm. The second strategy (ABA) consists of beads (A) welded at a distance of 14 to 18 mm from each other, so that a third bead (B) can be deposited in the space between. Claddings with the determined track spacing for AAA of 9 mm and ABA 18 mm were created in order to compare the resulting surface properties. The ABA cladding did not achieve a more uniform surface and less waviness than the AAA cladding.

Keywords: LDNA, cladding, waviness, welding strategy, high deposition rate

Introduction

Deposition welding processes are often used for cladding and repairing work pieces such as metal forming dies [1]. A wide range of deposition rates is represented with a wide variety of processes that are purely laser-based, purely arc-based or use a combination of laser radiation and welding arc. There are processes with low deposition rates in the range of 1 kg/h, which can achieve a high structure resolution, and on the other hand there are processes that achieve high deposition rates of up to 20 kg/h with considerably lower structure resolution. Laser-assisted double-wire welding with nontransferred arc (LDNA) developed at the Laser Zentrum Hannover e.V. with deposition rates of 5 to 21 kg/h is one of these processes. Due to the high deposition rate, the process is particularly well suited for coating large components or large surfaces, which are often found in the mining industry, for example [2]. The welding strategy investigated so far is based on the alignment of weld beads. Other strategies have not yet been investigated. This study deals with the comparison of different deposition strategies.

State of the art

For the production of claddings with a thickness of less than one millimeter up to several millimeters, cladding processes based on welding processes are used. The weld beads applied by these processes are usually not sufficient to cover the area to be cladded, so that several weld beads have to be applied next to each other with an overlap. [3] In claddings with high deposition rates, the surfaces often have a high degree of waviness and roughness, which is why machining is used after the cladding process to produce the required properties [4]. A conventional method for cladding is to use the GMAW process. This can be used in any welding position, is very reliable and, compared to pure laser processes, very effective in terms of energy use and costs. [5] The

process uses an electric arc that burns between a metal wire and the work piece, causing the wire to melt. As a result, there is a high thermal input into the component and the level of dilution of the cladding with the work piece is comparatively high. For this reason, there are approaches to reduce the heat input and the degree of dilution by using a process variant with a colder material transition. This variant is represented by the Cold Metal Transfer, for example. [6]

Another approach to reduce heat input into the work piece is the LDNA process developed by Barroi et al. The LDNA process uses a combination of an electric arc and a laser beam for cladding, whereby high deposition rates can be achieved. The high deposition rates result from the high melting potential of the electric arc, which burns between two wires that are continuously fed to each other at an angle. The laser radiation is used to enhance the bonding of the melt droplets falling onto the substrate. The laser radiation is precisely oscillated by a galvanometer scanner in the melt pool. [2] Further studies by Barroi et al. on the LDNA process consider the influence of the heat introduced into the process by the laser radiation. The radiation was oscillated through a 1D galvanometer scanner with a sinusoidal motion profile. It was shown that the sinusoidal function allows heat to be introduced at the points where it is needed to bond the melt without forming undercuts. Weld beads of AISI 316L on AISI 1024 were created. The evaluation was performed using micrographs and the best result was determined with an amplitude of 13.2 mm and a contact angle of 93° to the substrate normal. [7] Studies on the cladding of AISI 1024 components with AISI 316L were carried out by Barroi et al. The results show that claddings with a low number of bonding defects and without pores can be produced at a deposition rate of 7.5 kg/h. The degree of dilution is less than 5%. The bonding defects occur at the transition of the adjacent beads on the substrate surface, so that they have no influence on the function of the cladding. [8]

Further studies on the LDNA process by Bokelmann et al. investigate the influence of the position of the laser radiation in the melt pool on the resulting bead geometry. Parameters varied were the defocusing of the laser radiation, the position of the radiation in the met pool and the oscillation amplitude. The best weld beads were obtained with a defocusing of the laser beam of -1 mm below the focal point with a positioning of the laser beam of 3.5 mm in the melt pool against the welding direction with an oscillation amplitude in the range of 12.7 mm to 13.7 mm. [9] Bokelmann et al. investigated the weld bead geometry and the degree of dilution of the weld beads created with the LDNA process. A linear and convex oscillating form was investigated. The result is that a wider weld can be achieved with a convex oscillating form. On the other hand, the oscillating form has no significant influence on the dilution. [10]

Biester et al. were able to show that instead of a 2D galvanometer scanner, a beam shaping optic in the form of a line could be used to produce weld beads without undercutting. However, the weld beads could not be produced with the low level of dilution in contrast to using beam deflection. [11]

Koti, Powell and Voisey have investigated a new cladding strategy, 'ABA' cladding, using laser metal deposition with powder (LMD-P). A series of separate or only minimally overlapping parallel weld beads ('A' weld beads) were deposited to create the cladding. Between the 'A' weld beads, another weld bead ('B' weld bead) with adjusted parameters was deposited afterwards. The influence of the process parameters when using AISI 316L and Stellite 6 powders was investigated. The results show that with the new cladding strategy, the powder catchment rate and the coverage rate can be increased, and the microstructure and the degree of dilution can be predicted more accurately. [12] In another study by Koti et al. comparing ABA cladding with AAA cladding, the powder catchment rate and the influence of the distance of the ‘A’ weld beads, as well as the influence of the welding speed, were investigated. It was found that the melt pool geometry was asymmetrical for all weld beads after the initial weld bead for AAA cladding. Compared to AAA cladding, an increased powder catchment rate was found for ABA claddings. By increasing the

distance between the two ‘A’ weld beads, no influence of the catchment rate could be determined for ABA claddings. In contrast, an improvement was seen with AAA claddings. Increasing the welding speed was shown to have a small effect on melt pool size and catchment rate.[13]

Aims and perspective

This study focuses on the comparison of the different strategies for cladding. In the following, the findings on the resulting surface and subsurface properties are presented using the example of two different welding strategies, strategy AAA and strategy ABA. The following scientific questions are to be answered:

1. How does the strategy ABA affect the surface and subsurface properties of the cladding regarding
   a) Waviness
   b) Dilution?
2) How does the cladding produced with strategy ABA affect the amount of machining required to achieve the final geometry?

Materials and methods

In this study, claddings are produced with the LDNA process using AISI 316L material on an AISI 1024 substrate. The cladding material is used in wire form, each with a diameter of 1.2 mm. The substrate has a thickness of 15 mm. The surface was sandblasted and cleaned with isopropanol before the welding tests to ensure an even specimen preparation. The chemical composition of the materials used is shown in Table 1.

Table 1: Chemical composition of the investigated materials [14], [15]

	C	Si	Mn	P	S	Cr	Ni	Mo	Fe
AISI 1024	0.2	0.55	1.60	0.025	0.025	-	-	-	Bal.
AISI 316L	0.02	0.80	1.70	<0.02	<0.01	19.0	12.0	2.70	Bal.

The basic structure of the processing head consists of a torch holder, in which the wires are fed one on top of the other, and a 2D galvanometer scanner, which deflects the laser beam and oscillates it in the process. The principle is shown schematically in Figure 1.

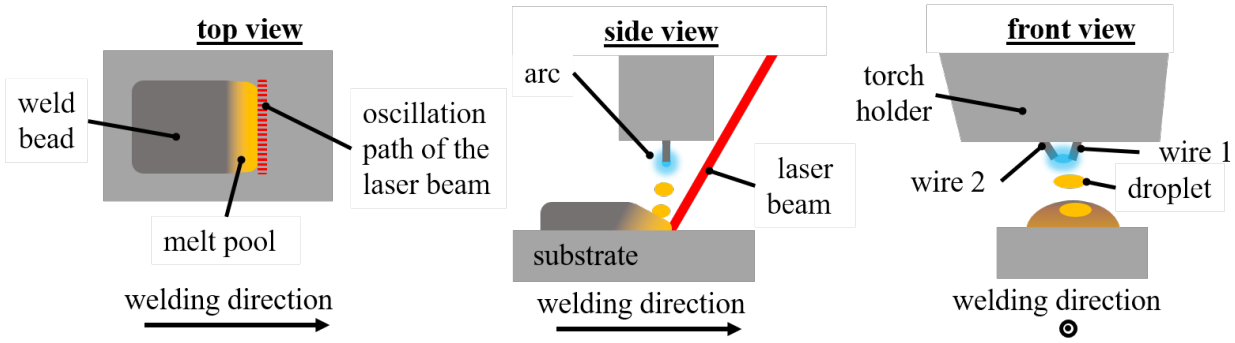

Figure 1: Principle of the LDNA process

The system components used to conduct the investigation consisted of the following. A HighPULSE 454 DW direct current welding source from *Merkle Schweißanlagen-Technik GmbH*, modified for the double-wire process. The laser beam source used is a TruDisk 16002 disk laser

from *Trumpf SE + Co. KG* with a maximum power of 16,000 W. Handling of the processing head was carried out by a 6-axis industrial robot KR60HA from *Kuka AG*. The processing head used is shown in Figure 2.

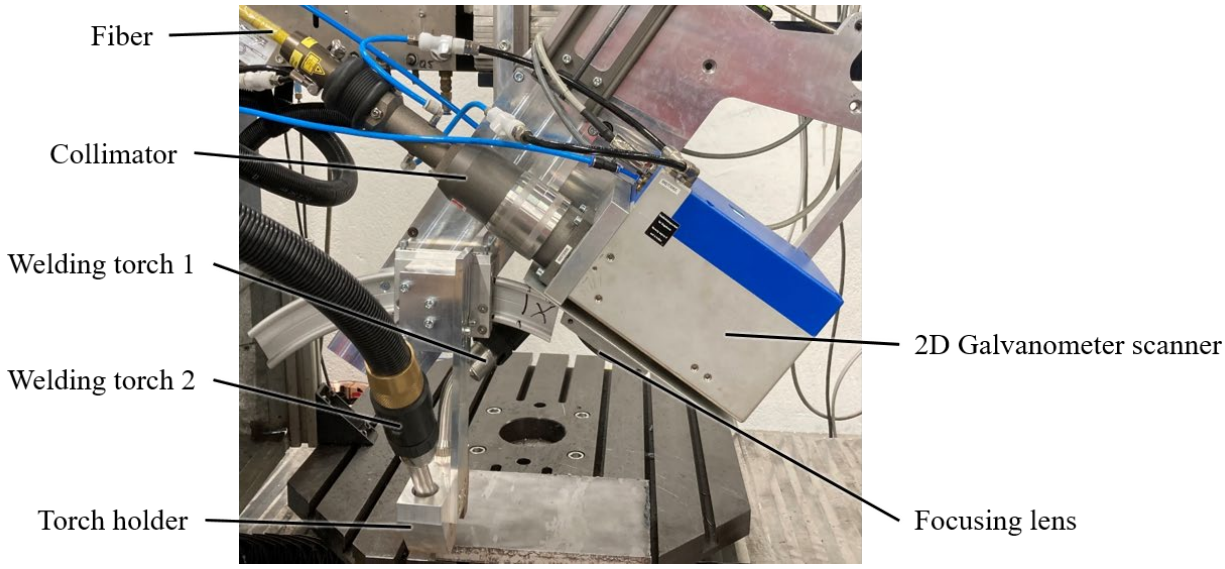

Figure 2: Processing head for the LDNA process

The laser radiation has a wavelength of 1030 nm. The laser radiation is guided to the process zone with a fiber that has a core diameter of 600 µm. The numerical aperture of the fiber is 0.1. The focal length of the collimator lens is 138 mm and the effective focal length of the focus lens is 300 mm.

The LDNA process is carried out with a shielding gas mixture of 82% CO_2 and 18% argon. The other process parameters, which are kept constant, are shown in Table 2.

Table 2: Parameters for the LDNA process

Parameter	**Unit**	
Welding current	A	245
Welding voltage	V	31.5
Wire feed rate 1	m/min	10
Wire feed rate 2	m/min	12
Welding speed	mm/min	600
Shielding gas flow rate	l/min	22
Laser power	W	1,000
Oscillation frequency	Hz	10
Oscillation amplitude	mm	13.2
Movement of laser focus	-	Sinusoidal function
Distance between torch holder and substrate	mm	15

Two different strategies are followed for the cladding. Firstly, the AAA strategy is used in which weld beads with an overlap are deposited next to each other. In the second strategy ABA, two weld beads are created without an overlap (A) and a third weld bead (B) is deposited between

the two previously deposited beads. All weld beads, both in AAA and ABA strategy are created with the same set of parameters. The principle of the welding strategies is shown in Figure 3.

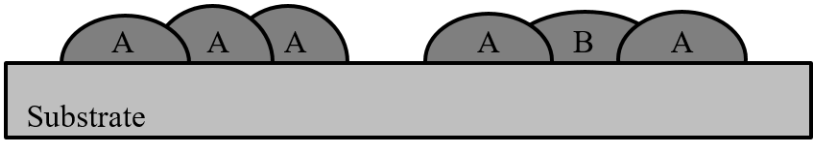

Figure 3: Principle of the welding strategies, strategy AAA on the left side and strategy ABA on the right side

In this study, the weld bead distance is first determined for the cladding. Specimens with three weld beads each and a length of 100 mm are generated for this purpose. Like the oscillation amplitude, the width of a weld bead is also about 13 mm, as this allows a good weld bead shape to be obtained as shown by Barroi et al. [7]. The parameter range is investigated between 7 mm to 9 mm for the determination of distance between weld beads for AAA cladding. The parameters result from overlap ratios between approx. 50% to approx. 30%. Previous empirical investigations have shown that the surfaces with the best properties are obtained in the selected range. For ABA cladding, the distance between the two 'A' weld beads is varied. A range from 14 mm to 18 mm is investigated. The distances are changed in increments of one millimeter. For statistical validation of the results, the experimental design is carried out with the help of design of experiments with the Software JMP from *SAS Institute GmbH* and with three repetitions per parameter set in randomized order.

After determining the best distances in the selected parameter range, claddings consisting of eleven weld beads will be created to determine the surface property waviness. In addition, the degree of dilution will be determined and compared.

The evaluation of waviness is based on a surface measurement of each weld bead with a Laser Scanning Microscope VK-X1100 from *Keyence Deutschland GmbH*, taken at a length of 50 mm. For the determination of the degree of dilution, the specimens are separated at a length of 50 mm. The specimens are then ground, polished and etched with V2A etchant. The images are taken with the same microscope as for the surface measurement.

Results and discussion

For the first part of the study, the AAA claddings, the micrographs are used to determine the total width and total height of the cladding. The total widths of the three deposited weld beads range from 28.1 mm to 32.8 mm. As expected, a significant correlation with a p-value of 0.0001 was found when statistically examining the dependence of the distance between weld beads on the total width of the weld structure. As the distance between the weld beads increases, the total width increases due to the increase in the distance. Similarly, the result is noticeable when examining the correlation of the distance between weld beads on the total height. The total height is significantly dependent on the distance between weld beads with a p-value of 0.0018. As the distance between weld beads increases, the total height decreases in the parameter space studied. This effect is due to the fact that the degree of overlap of the weld beads is greater at lower distance from the weld beads, which results in a higher buildup of the welded structure. The total height is in the range of 5.03 mm to 6.24 mm. Figure 4 shows an example of an AAA cladding with a distance between the weld beads of 9 mm. It can be seen that the weld beads are well bonded. The only visible bonding defect is in the transition area of two weld beads at the level of the substrate surface, which does not affect the function of the cladding.

Figure 4: Cross-section of an AAA cladding with a distance between the weld beads of 9 mm

Figure 5, on the top left side, shows the measured total heights and total widths versus the distance between weld beads. From the data, the trend and the significant correlation of the two parameters from the distance between weld beads can be seen. The evaluation of the waviness of the AAA claddings is based on the surface measurement of the weld structures. The evaluation yields values in a range from 764 µm to 1,325 µm. Figure 5, centered on the left side, shows the individual values of the measured waviness as well as the trend versus the distance between weld beads. The trend shows that the waviness decreases with increasing distance between weld beads. This correlation could be proven by a statistical calculation. With a p-value of 0.0233, there is a significant correlation between the waviness and the distance between weld beads. The waviness becomes lower due to the lower total height as well as the lower degree of overlap of the individual weld beads. The degree of dilution is determined on the basis of the transverse micrographs. For the determination, the surface areas of the weld structure above A_{above} and the surface areas of the welded material below the substrate surface A_{below} are determined and calculated by the following formula:

$$\text{Degree of dilution} = \frac{A_{above}}{A_{above} + A_{below}} \cdot 100\%$$

For the AAA claddings, the values of the degree of dilution are in the range of 8.1% to 12.4%. Figure 5, on the bottom left side, shows the degree of dilution and the trend plotted versus distance between weld beads. It can be seen that the degree of dilution increases with increasing distance between weld beads. The correlation is significant with a calculated p-value of 0.0052. The increasing degree of dilution with increasing distance between weld beads is because the degree of overlap between the individual weld beads decreases and that the thermal energy introduced by the process affects more the substrate instead of the previously applied weld bead. This results in greater dilution between the deposit material and the base material.

With the help of the correlations shown, a distance between weld beads of 9 mm is selected for the comparison of the welding strategies on the basis of the creation of a cladding for the AAA strategy. The requirement for a cladding to have as little waviness as possible, so that the degree of rework required is kept to a minimum, is the distance between weld beads selected. Another effect associated with this is that the cladding has a low overall height with a maximum width due to the choice of distance between weld beads. Only a higher degree of dilution has to be accepted in comparison to a low distance between weld beads.

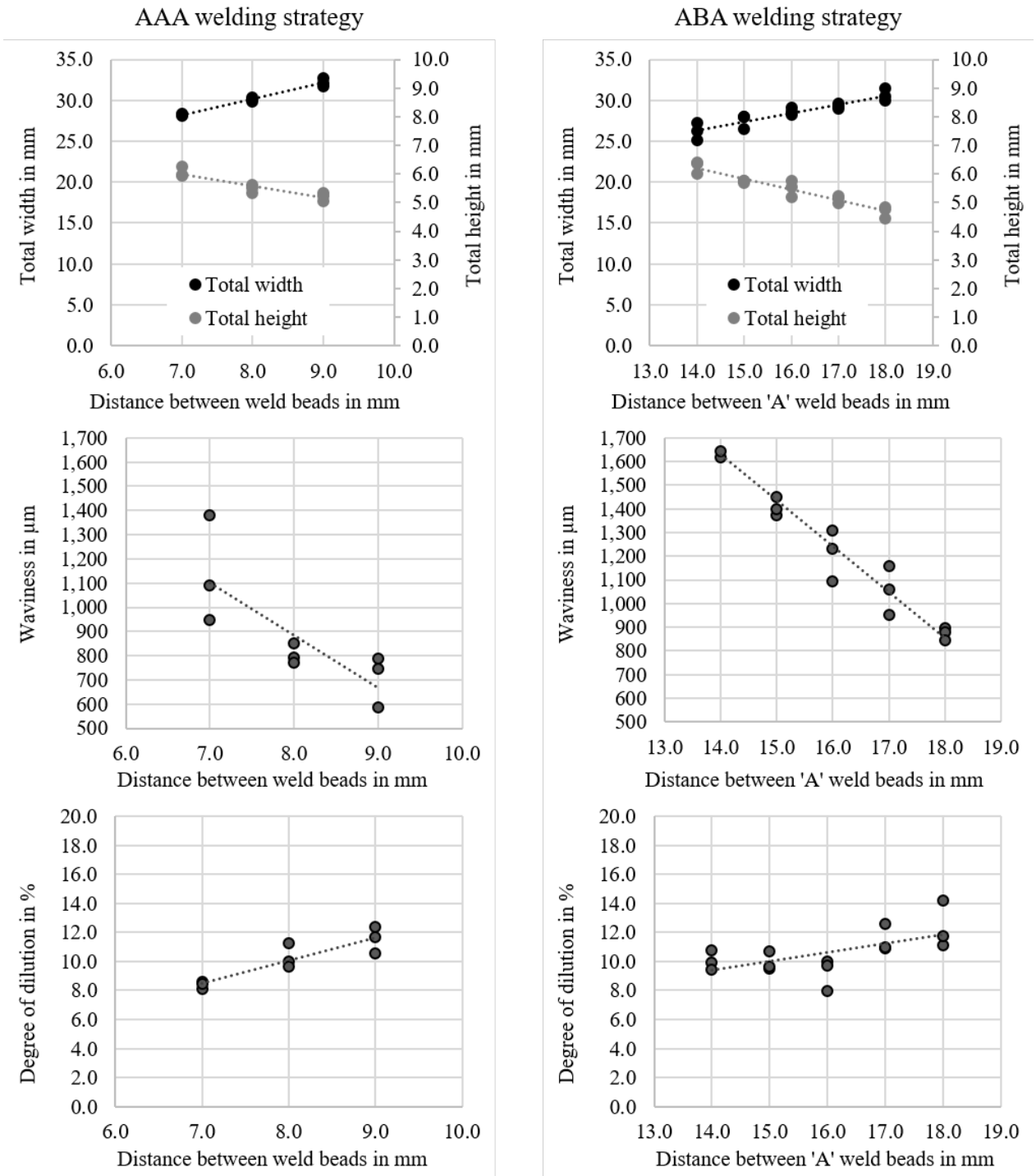

Figure 5: Diagrams for the AAA strategy (left) and the ABA strategy (right) of total height and total width versus distance between weld beads (top row), waviness versus distance between weld beads (middle row) and degree of dilution versus distance between weld beads (bottom row)

The cross-section images are also used to determine the total width for the second welding strategy investigated, ABA. The values determined for the total width of the ABA claddings with three weld beads range from 25.6 mm to 32.0 mm. The statistical test for a correlation between the total width and the distance between the 'A' weld beads is significant with a p-value of 0.0002. As the distance between the 'A' weld beads increases, the overall width of the weld structure increases,

as expected. The measured values of total heights range from 5.58 mm to 7.29 mm. The dependence of the total height on the distance between the 'A' weld beads is significant with a p-value of 0.0001. The smaller distance between the two 'A' weld beads leaves less room for the material of the 'B' weld bead to spread, therefore the weld bead builds up more, resulting in the higher total height. As the distance between the 'A' weld beads increases, the material deposited by the 'B' weld bead can better distribute between the previously deposited weld beads. Figure 6 shows a weld structure created using the ABA strategy with 18 mm distance between the two 'A' weld beads. Minimal bonding defects are evident at the intersection of the substrate surface with the surface of the 'A' weld bead and the 'B' weld bead on both sides. As with the cladding using the AAA strategy, the bonding defects do not affect the function of the cladding.

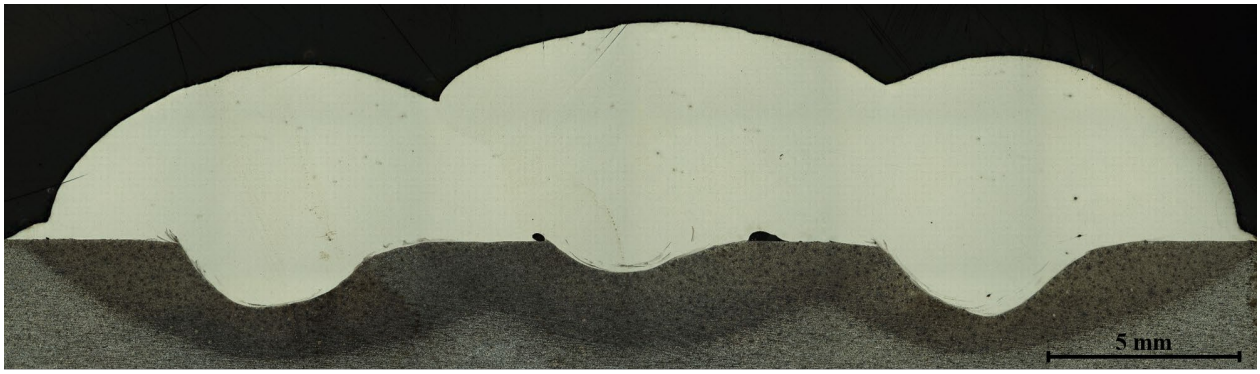

Figure 6: Cross-section of an ABA cladding with a distance between the 'A' weld beads of 18 mm

Figure 5, on the top right side, shows the total height and total width of the weld structures as a function of the distance between the 'A' weld beads. In addition, a trend is shown in each case. As expected, the measured values show a similar trend to the claddings created using the AAA strategy. The waviness is determined based on the surface measurements. The values determined range from 887 µm to 1,629 µm. A statistical correlation between the waviness and the distance between the 'A' weld beads could be demonstrated with a p-value of 0.0001. Figure 5, centered on the right side, presents the measured values of waviness and the trend of the data versus the distance between the 'A' weld beads. As the distance between the weld beads increases, the waviness of the weld structure decreases. This effect is due to the fact that the overlap of the 'B' weld bead with the 'A' weld beads decreases and thus the total height decreases and the waviness decreases at the same time. The degree of dilution of the ABA claddings is in the range of 8.0% to 14.2%. The statistical analysis shows a significant correlation between the degree of dilution and the distance between the 'A' weld beads. Figure 5, on the bottom ride side, shows the values of the degree of dilution plotted versus the distance between the 'A' weld beads. It is noticeable that for distances between 'A' weld beads of 14 mm to 16 mm, the degree of dilution remains relatively constant at around 10% and only starts to increase when the distance between 'A' weld beads exceeds 16 mm. This can be attributed to the fact that the 'B' weld bead does not generate a weld penetration into the substrate until the distance between the 'A' weld beads exceeds 17 mm, and is thus included in the evaluation for the degree of dilution. Prior to this, the bond of the 'B' weld bead is generated on the flanks therefore a considerably amount of energy is dissipating in the existing 'A' weld beads. In spite of the issue shown, a significant correlation between the degree of dilution and the distance between the 'A' weld beads can be calculated with a p-value of 0.0295.

Based on the same requirements for a cladding, 18 mm is chosen as the parameter for the distance between the 'A' weld beads for the comparison of the strategies. As with the AAA claddings, this is at the expense of the degree of dilution.

The comparison of claddings created with the selected distance between weld beads parameters, consisting of eleven weld beads, are shown in Figure 7. The grid-like pattern that can be seen results from the fact that individual images had to be stitched for the overview of the cladding. The upper part of Figure 7 shows the cladding created with the AAA strategy and the lower part of Figure 7 shows the cladding created with the ABA strategy. The AAA cladding has very good bonding with only a very small bonding error between the deposition material and the substrate surface. The ABA cladding has bonding defects also at the junction between the substrate surface and the deposited structure. As with the parameter determination, the weld defects form at the intersections between the flanks of the 'A' weld beads, the substrate surface and the 'B' weld beads. The bonding defects that occur in the cladding can be attributed to a non-optimal parameter set for the distance between the 'A' weld beads or to insufficient energy introduced by the laser radiation to ensure bonding. The occurrence of the bonding defect exclusively on the left side of the 'B' weld bead can be attributed to a non-symmetrical weld bead shape. In the future, an extension of the parameter space towards larger distances between the 'A' weld beads should be investigated. This may lead to an improvement in the bond but also to an improvement in the waviness with respect to the exaggeration of the maxima of the 'B' weld beads compared to the maxima of the 'A' weld beads. Another approach is to increase the laser power so that the additional energy can be used to achieve a bond. Furthermore, an adaptation of the oscillation form of the laser radiation for the 'B' weld beads would be conceivable.

The AAA cladding has a total width of 95.9 mm with a total height of 5.69 mm. The waviness was determined to be 396 µm. The degree of dilution is 9.4%. The ABA cladding has a total width of 103.8 mm with a total height of 5.17 mm. The waviness is 477 µm. The determined degree of dilution is 11.8%.

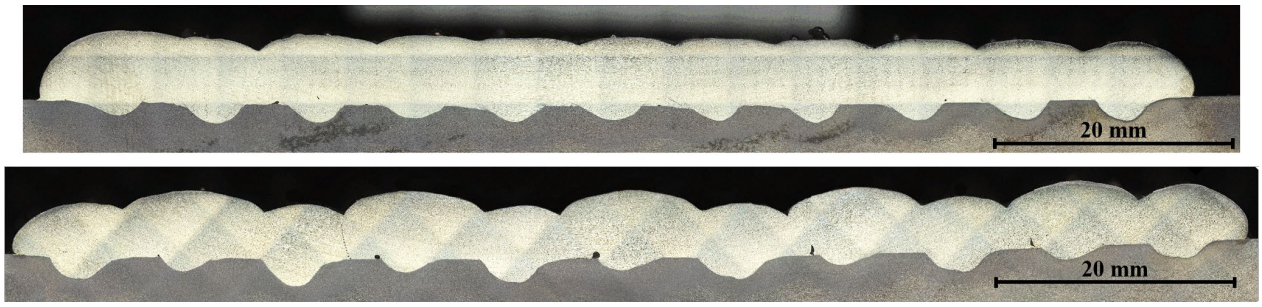

Figure 7: Cladding consisting of eleven weld beads created with the AAA strategy (top) and the ABA strategy (bottom)

Table 3 shows an overview of the determined values for the claddings consisting of eleven weld beads. When comparing the determined values of the claddings, it can be seen that a narrower and slightly higher cladding was obtained with the AAA strategy than with the ABA strategy. The measured waviness differs, with the waviness obtained with the AAA strategy producing a better waviness. There is a slight difference in the results obtained with the degree of dilution. The degree of dilution is lower with the AAA cladding at 9.4% than with the ABA cladding at 11.8%.

Table 3: Summary of the results obtained when comparing the welding strategies based on the created claddings with eleven weld beads each

Parameter	Unit	Welding strategy AAA	Welding strategy ABA
Total width	mm	95.9	103.8
Total height	mm	5.69	5.17
Waviness	µm	396	477
Degree of dilution	%	9.4	11.8

Comparing the larger claddings produced with the measured values for the waviness and degree of dilution when determining the distance between the weld beads for the different strategies, there are in some cases larger deviations. For the AAA strategy, an average degree of dilution of 11.6% is obtained with a distance between the weld beads of 9 mm. This is slightly higher than the achieved degree of dilution of the larger AAA cladding of 9.4%. A bigger difference lies in the waviness, which for the small cladding consisting of three wed beads has an average waviness of 850 µm. The larger cladding has a considerably lower waviness of 396 µm. The situation is similar for the ABA cladding. The average waviness of the cladding consisting of three weld beads is 1035 µm, whereas the waviness for the larger cladding is 477 µm. Likewise, there is a difference in the degree of dilution. For the small cladding, an average degree of dilution of 12.3% was determined. For the larger cladding, a smaller degree of dilution of 11.8% was determined.

The waviness of the ABA cladding is greater than the waviness of the AAA cladding. In the study by Koti et al. an improvement in surface properties was observed for the ABA claddings compared to the AAA claddings. This improvement was obtained by adjusting the welding parameters for depositing the 'B' weld beads. The ABA cladding created in this study is created with a set of welding parameters, so a further study should investigate whether adjusting the parameters for the 'B' weld beads also leads to an improvement in this process. In Figure 7 below, it can be seen that the 'B' weld beads have an elevation compared to the 'A' weld beads. This elevation had not occurred to the same extent in the previous parameter determinations, so a further line of investigation is to further increase the distance between weld beads for the 'A' weld beads in the ABA strategy in order to reduce or eliminate the elevation.

Conclusion and outlook

Two different welding strategies for creating claddings with the LDNA process were investigated. One is the conventional AAA welding strategy, in which the weld beads are deposited adjacent to each other. On the other hand, the ABA welding strategy, in which a ‘B’ weld bead is welded between two previously deposited ‘A’ weld beads. For the comparison of two claddings, 9 mm was chosen as the distance between weld beads parameter for the AAA cladding. The ABA cladding was created with a parameter of 18 mm for the distance between the 'A' weld beads. The surface properties obtained with the selected parameters have a waviness of 477 µm, which is higher than the AAA cladding. Similarly, the degree of dilution for the ABA cladding is 11.8%, 2.4% higher than the degree of dilution for the AAA cladding. For the ABA claddings, bonding defects occurred at regular intervals, whereas for the AAA cladding, only a small defect is evident. With the investigated parameter space, no minimization of rework, for example, a milling rework can be achieved with the ABA welding strategy, so that further investigations must be carried out to optimize the parameters. In addition, optimization is necessary to prevent bonding defects.

One approach for further investigation is to expand the parameter space for the distance between the two 'A' weld beads in the ABA strategy. In addition, the approach of adjusting the welding parameters for the creation of the 'B' weld beads could be pursued to improve the surface properties of the ABA cladding. Furthermore, another approach to optimization is to adjust the laser oscillation form and the laser oscillation strategy.

Acknowledgements

The results presented in this paper were obtained within the project “Flexible and efficient generation of unique ship components using an innovative laser-assisted additive manufacturing process (FLEXIGEN)” (No. 03SX517C). The authors acknowledge the Federal Ministry for Economic Affairs and Climate Action for their financial support of this project.

Supported by:

on the basis of a decision
by the German Bundestag

References

[1] S. Nowotny, “Beschichten, Reparieren und Generieren durch Präzisions-Auftragschweißen mit Laserstrahlen,” *Vakuum in Forschung und Praxis*, vol. 14, no. 1, p. 33, Feb. 2002, doi: 10.1002/1522-2454(200202)14:1<33::AID-VIPR33>3.0.CO;2-X.

[2] A. Barroi, J. Hermsdorf, U. Prank, and S. Kaierle, “A Novel Approach for High Deposition Rate Cladding with Minimal Dilution with an Arc – Laser Process Combination,” *Phys Procedia*, vol. 41, pp. 249–254, 2013, doi: 10.1016/j.phpro.2013.03.076.

[3] C. Leyens and E. Beyer, “Innovations in laser cladding and direct laser metal deposition,” in *Laser Surface Engineering*, Elsevier, 2015, pp. 181–192. doi: 10.1016/B978-1-78242-074-3.00008-8.

[4] M. Merklein, D. Junker, A. Schaub, and F. Neubauer, “Hybrid additive manufacturing technologies - An analysis regarding potentials and applications,” *Phys Procedia*, vol. 83, pp. 549–559, 2016, doi: 10.1016/j.phpro.2016.08.057.

[5] M. Kumar Saha and S. Das, “Gas Metal Arc Weld Cladding and its Anti-Corrosive Performance- A Brief Review,” *Athens Journal of Technology & Engineering*, vol. 5, no. 2, pp. 155–174, 2018, doi: 10.30958/ajte.5-2-4.

[6] Y. Ali, P. Henckell, J. Hildebrand, J. Reimann, J. P. Bergmann, and S. Barnikol-Oettler, “Wire arc additive manufacturing of hot work tool steel with CMT process,” *J Mater Process Technol*, vol. 269, pp. 109–116, Jul. 2019, doi: 10.1016/j.jmatprotec.2019.01.034.

[7] A. Barroi, J. Amelia, J. Hermsdorf, S. Kaierle, and V. Wesling, “Influence of the laser and its scan width in the LDNA surfacing process,” *Phys Procedia*, vol. 56, no. C, pp. 204–210, 2014, doi: 10.1016/j.phpro.2014.08.164.

[8] A. Barroi, F. Zimmermann, J. Hermsdorf, S. Kaierle, V. Wesling, and L. Overmeyer, “Evaluation of the laser assisted double wire with nontransferred arc surfacing process for cladding,” *J Laser Appl*, vol. 28, no. 2, p. 022306, 2016, doi: 10.2351/1.4944001.
[9] T. Bokelmann *et al.*, “Influence of the laser beam parameters in the laser assisted double wire welding with nontransferred arc process on the seam geometry of generatively manufactured structures,” *J Laser Appl*, vol. 33, no. 4, p. 042044, 2021, doi: 10.2351/7.0000521.
[10] T. Bokelmann *et al.*, “Influence of laser spot oscillation parameters on the seam geometry and dilution in in the LDNA process,” *Procedia CIRP*, vol. 111, pp. 185–189, 2022, doi: 10.1016/j.procir.2022.08.043.
[11] K. Biester, A. Barroi, T. Bokelmann, M. Lammers, J. Hermsdorf, and S. Kaierle, “High deposition rate welding with a laser line optics with the laser-assisted double- wire deposition welding process with nontransferred arc,” *Journal of Laser Application*, vol. 042010, no. 34, 2022, doi: 10.2351/7.0000758.
[12] D. Koti, J. Powell, and K. T. Voisey, “Improving laser cladding productivity with ‘ABA’ cladding,” *Procedia CIRP*, vol. 111, no. September, pp. 205–209, 2022, doi: 10.1016/j.procir.2022.08.048.
[13] D. Koti, J. Powell, H. Naesstroem, and K. T. Voisey, “Powder catchment efficiency in laser cladding (directed energy deposition). An investigation into standard laser cladding and the ABA cladding technique,” *J Laser Appl*, vol. 35, no. 1, p. 012025, 2023, doi: 10.2351/7.0000904.
[14] Salzgitter Flachstahl GmbH, “S355J2,” 2010. https://www.salzgitter-flachstahl.de/fileadmin/mediadb/szfg/informationsmaterial/produktinformationen/warmgewalzte_produkte/deu/S355J2.pdf
[15] Rotek Handels GmbH, “Draht-/Stabelektrode - E316L/1.4430 zum Schweißen nichtrostender und kaltzäher austenitischer Stähle,” 2008. https://media.rotek.at/aalg/schweissen/werkstoffe/MIG-WIG_E316L-1.4430_Datenblatt_Rotek_de.pdf